

Hidden bifurcations and attractors in nonsmooth dynamical system

Mike R. Jeffrey

*Engineering Mathematics, University of Bristol, Merchant Venturer's Building,
Bristol BS8 1UB, UK, email: mike.jeffrey@bristol.ac.uk*

(Dated: November 4, 2015)

We investigate the role of hidden terms at switching surfaces in piecewise smooth vector fields. Hidden terms are zero everywhere except at the switching surfaces, but appear when blowing up the switching *surface* into a switching *layer*. When discontinuous systems do surprising things, we can often make sense of them by extending our intuition for smooth system to the switching layer. We illustrate the principle here with a few attractors that are hidden inside the switching layer, being evident in the flow, despite not being directly evident in the vector field outside the switching surface. These can occur either at a single switch (where we will introduce hidden terms somewhat artificially to demonstrate the principle), or at the intersection of multiple switches (where hidden terms arise inescapably). A more subtle role of hidden terms is in bifurcations, and we revisit some simple cases from previous literature here, showing that they exhibit degeneracies inside the switching layer, and that the degeneracies can be broken using hidden terms. We illustrate the principle in systems with one or two switches.

I. INTRODUCTION

If a smoothly evolving system is interrupted by sudden jumps at a definite threshold, we may model it with a vector field that is smooth except at some *switching surface*. The seminal theory of such *piecewise smooth* vector fields was set out by Filippov [5], and began the systematic extension of standard smooth dynamical systems theory to admit isolated discontinuities (the relation to Krasovskij, Hermes, Gel'fand-Leonov-Yakubovich, and Aizerman-Pyatnitskiy definitions can be found in [9, 15]). Filippov showed how to solve a vector field across a discontinuity, giving, in most situations of interest, a well defined and deterministic flow. Utkin applied this to introduce *sliding modes* for electronic switching (or *variable structure* control) [3, 28, 29], and alongside growing uses in contact mechanics and the life sciences [2, 16, 23, 30], dynamical systems theory has been extended vastly to categorize the attractors and bifurcations induced by discontinuity [1, 5, 6, 18].

Progress in piecewise smooth theory and applications has relied heavily on treating the transition at the switching threshold as a true discontinuity, that is, as an abrupt switch in the value (or derivatives) of the vector field at a definite hypersurface in state or phase space. It is possible,

and sometimes necessary, to peer inside the discontinuity, to blow up the switching *surface* into a switching *layer*, revealing the fast dynamics of transition through the discontinuity. This can reveal terms in the vector field or its flow that are important inside the discontinuity, but are not directly discernible from outside the switching surface, and these are called *hidden* terms. To try and open up this field of inquiry, we present here novel oscillatory and chaotic attractors made possible by hidden terms, and we present bifurcations that can only be made sense of via hidden dynamics.

Rather than make a fully detailed treatment of each case, in this expository paper we give examples showing the typical role of hidden terms, aimed at providing a basis for more complete classification studies in the future. Normal forms or topological classification schemes do not yet exist which take account of the switching layer, and given some uncertainty in piecewise smooth theory concerning such notions (see e.g. [10]), a preliminary exploration such as we give here is warranted. The elementary behaviours we show will merely hint at the zoo of singularities and bifurcations that remain to be studied, and invite more detailed and rigorous studies of the examples given.

We illustrate the role of hidden terms in two parts. First we present attractors that are hidden inside the switching layer, whose existence cannot be inferred from the system outside the switching surface, but are evident in the system's dynamics. Secondly we study a few bifurcations that appear in standard literature, showing that they possess degeneracies inside the switching layer which require hidden terms to break. In some cases, revealing hidden dynamics inside the switching layer can help make sense of changes of attractivity. We will show examples where equilibria appear to change attractivity abruptly, without any exchange of attractivity with the environment via e.g. the creation or destruction of a limit cycle, and we show that a conventional, but hidden, bifurcation is actually responsible.

We first briefly review the key elements of sliding modes and switching layers in section II. Then in section III we describe novel oscillatory dynamics caused by hidden terms, beginning with relaxation oscillations inside a single switch, and then reviewing two cases from recent literature on multiple switches, namely limit cycles induced by 'cross-talk' between a pair of switches, and a Lorenz attractor hidden inside the intersection of three switches. In section IV we re-consider two bifurcations that have appeared in classifications of planar vector fields with a single switch, revealing their degeneracies, and the hidden dynamics that resolves them, and review an important case of hidden bifurcation induced by multiple switches. Some closing remarks are made in section V.

II. THE PIECEWISE SMOOTH APPROACH

We study systems of ordinary differential equations, defined by smooth vector which take different values \mathbf{f}^i on adjacent domains \mathcal{R}_i ,

$$\dot{\mathbf{x}} = \{ \mathbf{f}^i(\mathbf{x}) \quad \text{for} \quad \mathbf{x} \in \mathcal{R}_i, i \in \mathcal{I} \} ,$$

where \mathcal{I} is some set of m different labels (e.g. the integers $1, 2, \dots, m$, or, as we shall use later, a binary representation of them). The boundaries between regions form a *switching surface*, which we will assume is formed by a set of transversal hypersurfaces $h_j(\mathbf{x}) = 0$ for $j = 1, 2, \dots, r$, allowing the system to be expressed as

$$\dot{\mathbf{x}} = \mathbf{f}(\mathbf{x}; \boldsymbol{\lambda}) , \quad \lambda_i = \text{sign}(h_i(\mathbf{x})) , \quad (1)$$

where $\mathbf{x} = (x_1, x_2, \dots, x_n)$, $\mathbf{f} = (f_1, f_2, \dots, f_n)$, $\boldsymbol{\lambda} = (\lambda_1, \lambda_2, \dots, \lambda_r)$, for integers $n \geq r > 0$, where $m = 2^r$. Each vector field $\mathbf{f}(\mathbf{x}; \boldsymbol{\lambda})$ or $\mathbf{f}^i(\mathbf{x})$ can be assumed to be smooth in \mathbf{x} . Outside the switching surface, where all h_j are nonzero, the system (1) therefore has smooth and unique solutions. Extending these solutions across the switching surface requires a more precise definition than (1).

A. Dynamics in the switching layer

At a single switching surface given by $h_1(\mathbf{x}) = 0$, the system (1) becomes

$$\dot{\mathbf{x}} = \mathbf{f}(\mathbf{x}; \lambda_1) , \quad \lambda_1 = \text{sign}(h_1(\mathbf{x})) , \quad (2)$$

and following [5, 12] we extend this across $h_1 = 0$ by writing

$$\dot{\mathbf{x}} = \mathbf{f}(\mathbf{x}; \lambda_1) = \frac{1 + \lambda_1}{2} \mathbf{f}^+(\mathbf{x}) + \frac{1 - \lambda_1}{2} \mathbf{f}^-(\mathbf{x}) + (\lambda_1^2 - 1) \mathbf{g}(\mathbf{x}; \lambda_1) , \quad (3)$$

with $\lambda_1 = \text{sign}(h_1)$ for $h_1 \neq 0$, and $\lambda_1 \in (-1, +1)$ for $h_1 = 0$, for some smooth vector fields \mathbf{f}^+ , \mathbf{f}^- , and \mathbf{g} . Outside the switching surface the vector field on the righthand side is simply $\mathbf{f}^+(\mathbf{x}) \equiv \mathbf{f}(\mathbf{x}; +1)$ (for $h_1 > 0$) or $\mathbf{f}^-(\mathbf{x}) \equiv \mathbf{f}(\mathbf{x}; -1)$ (for $h_1 < 0$), consistent with (1). The vector field \mathbf{g} affects the system only on $h_1 = 0$, and is not fixed by comparison with (1). In this paper we will demonstrate when such a term is necessary.

Examples of the way \mathbf{g} may affect physical systems were suggested in [12, 14], and the nonlinear dependence on λ_1 introduced by \mathbf{g} is shown to be necessary for the structural stability of certain

common singularities in [13]. In this paper we explore these ideas more widely by studying the role of hidden terms in attractors and in bifurcations.

The dynamics of λ_1 , namely the transition of λ_1 between ± 1 at the switching surface, is induced by the change in h_1 as it passes through zero, which suggests defining the dynamics of λ_1 as

$$\lambda_1' = \mathbf{f}(\mathbf{x}; \lambda_1) \cdot \nabla h_1(\mathbf{x}) \quad \text{for } \lambda_1 \in (-1, +1) , \quad (4)$$

where the prime denotes differentiation with respect to an instantaneous transition timescale, $\tau = t/\varepsilon$, for infinitesimal positive constant ε . Combined with the original system $\dot{\mathbf{x}} = \mathbf{f}(\mathbf{x}; \lambda_1)$, and taking coordinates in which $x_1 = h_1$, the result is a two timescale system on the switching surface,

$$\left. \begin{aligned} \lambda_1' &= f_1(0, x_2, \dots, x_n; \lambda_1) \\ (\dot{x}_2, \dots, \dot{x}_n) &= (f_1(0, x_2, \dots, x_n; \lambda_1), \dots, f_n(0, x_2, \dots, x_n; \lambda_1)) \end{aligned} \right\} \text{ on } x_1 = 0 . \quad (5)$$

This defines dynamics on $\lambda_1 \in (-1, +1)$ and $(x_2, \dots, x_n) \in \mathbb{R}^{n-1}$, which we call the *switching layer*, and we call (5) the *switching layer system*.

Equilibria of the one-dimensional subsystem (4), if they exist, form *sliding modes* which satisfy

$$\left. \begin{aligned} 0 &= f_1(0, x_2, \dots, x_n; \lambda_1) \\ (\dot{x}_2, \dots, \dot{x}_n) &= (f_1(0, x_2, \dots, x_n; \lambda_1), \dots, f_n(0, x_2, \dots, x_n; \lambda_1)) \end{aligned} \right\} \text{ on } x_1 = 0 . \quad (6)$$

These evolve on the manifold

$$\mathcal{M}^S = \{(\lambda, x_2, \dots, x_n) \in (-1, +1) \times \mathbb{R}^{n-1} : f_1(0, x_2, \dots, x_n; \lambda) = 0\} . \quad (7)$$

This is an invariant manifold of the switching layer system (5) everywhere that \mathcal{M}^S is normally hyperbolic, that is, excepting the set where $\frac{\partial f_1}{\partial \lambda} = 0$, namely

$$\mathcal{L} = \left\{ (\lambda, x_2, \dots, x_n) \in \mathcal{M}^S : \frac{\partial}{\partial \lambda} f_1(0, x_2, \dots, x_n; \lambda) = 0 \right\} . \quad (8)$$

These principles form the basis all of the analysis to be carried out below. We shall also apply them to systems with multiple switches, for which they are easily extended as follows. At a point where r switching surfaces intersect, given by $h_1 = h_2 = \dots = h_r = 0$, the combination (3) generalises (see [11]) to

$$\dot{\mathbf{x}} = \mathbf{f}(\mathbf{x}; \boldsymbol{\lambda}) = \sum_{p_1, \dots, p_r = \pm} \lambda_1^{(p_1)} \dots \lambda_r^{(p_r)} \mathbf{f}^{p_1 \dots p_r}(\mathbf{x}) + \Gamma(\mathbf{x}; \boldsymbol{\lambda}) , \quad \lambda_i^{(\pm)} = \frac{1 \pm \lambda_i}{2} . \quad (9)$$

where $\boldsymbol{\lambda} = (\lambda_1, \lambda_2, \dots, \lambda_r)$, where $\mathbf{f}^{\pm \dots \pm}$ are 2^r smooth vector fields, each applying on one of the regions \mathcal{R}_i for $i = 1, 2, 3, \dots, 2^r$. The vector field Γ generalises the hidden term $(\lambda_1^2 - 1)\mathbf{g}$ from (3), satisfying

$$h_1 h_2 \dots h_r \Gamma(\mathbf{x}; \boldsymbol{\lambda}) = 0 , \quad (10)$$

so that Γ is only nonzero if one or more of the h_j vanishes. Extending (5), we take coordinates such that $x_j = h_j$ for $j = 1, 2, \dots, r$, and form a switching layer system by writing

$$\left. \begin{aligned} (\lambda'_1, \dots, \lambda'_r) &= (f_1(\mathbf{x}; \boldsymbol{\lambda}), \dots, f_r(\mathbf{x}; \boldsymbol{\lambda})) \\ (\dot{x}_{r+1}, \dots, \dot{x}_n) &= (f_{r+1}(\mathbf{x}; \boldsymbol{\lambda}), \dots, f_n(\mathbf{x}; \boldsymbol{\lambda})) \end{aligned} \right\} \text{ on } x_1 = \dots = x_r = 0, \quad (11)$$

the switching layer being the region

$$(\lambda_1, \dots, \lambda_r) \in (-1, +1)^r, \quad (x_{r+1}, \dots, x_n) \in \mathbb{R}^{n-r}.$$

The primes on the lefthand side of (11) denote differentiation with respect to instantaneous transition timescales. These timescales need not be identical (as we shall see in section IIIB), so for infinitesimal constants $\varepsilon_1, \varepsilon_2, \dots, \varepsilon_r$, the primes denote

$$\lambda'_1 \equiv \varepsilon_1 \frac{d}{dt}, \quad \lambda'_2 \equiv \varepsilon_2 \frac{d}{dt}, \quad \dots, \quad \lambda'_r \equiv \varepsilon_r \frac{d}{dt}. \quad (12)$$

If equilibria of the primed subsystem exist, the λ_j 's collapse in fast time to values given by

$$\left. \begin{aligned} (0, \dots, 0) &= (f_1(\mathbf{x}; \boldsymbol{\lambda}), \dots, f_r(\mathbf{x}; \boldsymbol{\lambda})) \\ (\dot{x}_{r+1}, \dots, \dot{x}_n) &= (f_{r+1}(\mathbf{x}; \boldsymbol{\lambda}), \dots, f_n(\mathbf{x}; \boldsymbol{\lambda})) \end{aligned} \right\} \text{ on } x_1 = \dots = x_r = 0. \quad (13)$$

Solutions of (13) are *codimension r sliding modes*, defining dynamics sliding along the intersection of r switching surfaces. Sets of points where sliding modes exist form manifolds

$$\mathcal{M}^S = \left\{ \begin{array}{l} (\lambda_1, \dots, \lambda_r) \in (-1, +1)^r \\ (x_{r+1}, \dots, x_n) \in \mathbb{R}^{n-r} \end{array} : \begin{array}{l} f_i(0, \dots, 0, x_{r+1}, \dots, x_n; \lambda_1, \dots, \lambda_r) = 0 \\ \text{for } i = 1, \dots, r \end{array} \right\}. \quad (14)$$

These are normally hyperbolic except at points on a set

$$\mathcal{L} = \left\{ (\lambda_1, \dots, \lambda_r, x_{r+1}, \dots, x_n) \in \mathcal{M}^S : \det \left| \frac{\partial(f_1, \dots, f_r)}{\partial(\lambda_1, \dots, \lambda_r)} \right| = 0 \right\}, \quad (15)$$

so the sets $\mathcal{M}^S \setminus \mathcal{L}$ form invariant manifolds of the flow, on which the sliding modes exist.

For any number of switches r , equilibria of the full switching layer system (where the righthand side of (11) vanishes), correspond to equilibria of the sliding system (13) (sometimes called *pseudoequilibria* in the piecewise smooth dynamics literature). Their stability can be studied by finding the jacobian of the vector field (11) evaluated at the fixed points, however it is important to make the timescales implicit in the prime notation explicit using (12), and the jacobian evaluates as

$$\left(\begin{array}{cc} \frac{\partial(\dot{\lambda}_1, \dots, \dot{\lambda}_r)}{\partial(\lambda_1, \dots, \lambda_r)} & \frac{\partial(\dot{\lambda}_1, \dots, \dot{\lambda}_r)}{\partial(x_{r+1}, \dots, x_n)} \\ \frac{\partial(\dot{x}_{r+1}, \dots, \dot{x}_n)}{\partial(\lambda_1, \dots, \lambda_r)} & \frac{\partial(\dot{x}_{r+1}, \dots, \dot{x}_n)}{\partial(x_{r+1}, \dots, x_n)} \end{array} \right) = \left(\begin{array}{cc} \frac{\partial(\varepsilon_1^{-1} f_1, \dots, \varepsilon_r^{-1} f_r)}{\partial(\lambda_1, \dots, \lambda_r)} & \frac{\partial(\varepsilon_1^{-1} f_1, \dots, \varepsilon_r^{-1} f_r)}{\partial(x_{r+1}, \dots, x_n)} \\ \frac{\partial(f_{r+1}, \dots, f_n)}{\partial(\lambda_1, \dots, \lambda_r)} & \frac{\partial(f_{r+1}, \dots, f_n)}{\partial(x_{r+1}, \dots, x_n)} \end{array} \right). \quad (16)$$

These elements, equations (9)-(11) and the concepts (13)-(16) derived from them, form the basis of everything that follows.

Each of the following examples is simple enough that we can sketch the piecewise smooth flows (9) for $\lambda_i = \text{sign}(h_i)$, the switching layer flows (11) for $h_i = 0$, and the sliding dynamics (13) on manifolds (14). A stability analysis of any equilibria in the switching layer proceeds from finding the jacobian (16).

III. HIDDEN SWITCHING ATTRACTORS

A *hidden attractor of switching* is a local or global attractor of the dynamical system, at least part of which lies inside the switching surface, but whose existence is not apparent from an inspection of the vector fields outside the switching surface. (The term should not be confused with the ‘hidden attractors’ of Leonov – attractors that are difficult to locate due to the form of their basins of attraction [19]). Novel attractors at the intersection of two or three switches have been reported in [8, 21], and hint at the range of non-trivial phenomena that may arise from such examples, so we review these briefly here. We begin, however, with an example of a planar system with a single switch.

A. Hidden van der Pol oscillator

The system

$$(\dot{x}_1, \dot{x}_2) = \left(\frac{1}{10}x_2 + \lambda - 2\lambda^3, -\lambda \right) \quad \text{where } \lambda = \text{sign}(x_1), \quad (17)$$

is deceptively simple for $x_1 \neq 0$,

$$(\dot{x}_1, \dot{x}_2) = \begin{cases} \left(\frac{1}{10}x_2 - 1, -1 \right) & \text{if } x_1 > 0, \\ \left(\frac{1}{10}x_2 + 1, +1 \right) & \text{if } x_1 < 0, \end{cases} \quad (18)$$

illustrated in figure 1(i). The surface $x_1 = 0$ is attracting.

In (17) we have a nonlinear switching term $\lambda - 2\lambda^3 = -\lambda + 2\lambda(1 - \lambda^2)$, the latter part constituting a ‘hidden term’ since it vanishes outside $x_1 = 0$. In the typical convex method (usually called a *Filippov system* [1, 5, 18]) we would ignore the hidden term, writing $(\dot{x}_1, \dot{x}_2) = \left(\frac{1}{10}x_2 - \lambda, -\lambda \right)$ consistent with (18), and then we would find that the point $x_1 = x_2 = 0$ is a simple attractor. We shall look instead at the effect of including the nonlinear dependence on λ .

The switching layer system, obtained by substituting (17) into (5), reveals a van der Pol oscillator,

$$(\lambda', \dot{x}_2) = \left(\frac{1}{10}x_2 + \lambda - 2\lambda^3, -\lambda \right) \quad \text{for } x_1 = 0, \quad \lambda \in (-1, +1). \quad (19)$$

The switching parameter λ thus undergoes relaxation oscillations, hidden inside $x_1 = 0$, shown in figure 1(ii). The relaxation oscillations cause λ to fluctuate inside the layer $\lambda \in (-1, +1)$, and

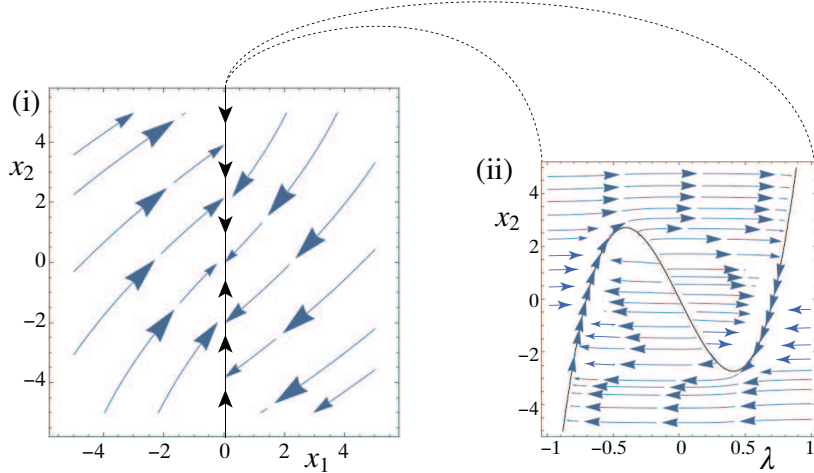


FIG. 1: Simulations of (17) showing: (i) the flow in the (x_1, x_2) plane, (ii) the flow inside $x_1 = 0$ given by (19).

cause x_2 to fluctuate between the folds of the curve $\frac{1}{10}x_2 = 2\lambda^3 - \lambda$. The oscillations in x_2 are on the normal timescale of the system (t rather than $\tau = t/\varepsilon$ from (4)). In figure 2(i) we plot the resulting graphs of x_2 and λ against time, and in (ii) a trajectory is simulated in the space of x_1, x_2, λ .

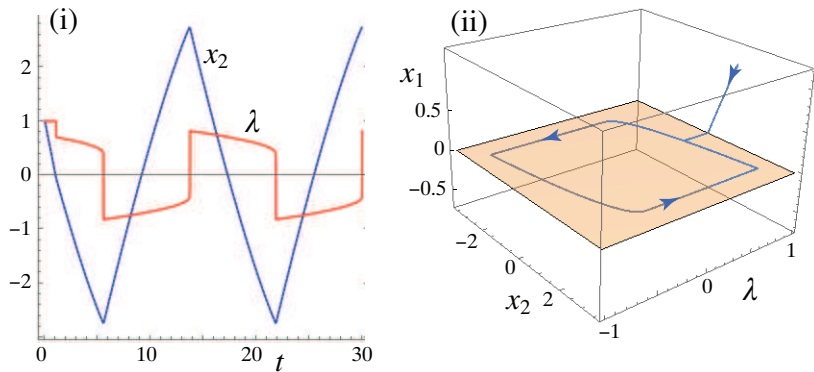


FIG. 2: Simulations revealing the hidden dynamics of (17): (i) graphs of the variable x_2 and λ , (ii) the corresponding orbit in the space of (x_1, x_2, λ) , with the switching surface at $x_1 = 0$.

In this example, oscillations inside the switching surface arise due to nonlinear dependence on the switching parameter $\lambda = \lambda_1$, creating a hidden van der Pol oscillator that affects the sliding

dynamics. If we have multiple switches then similar phenomena occur with only linear dependence on the individual switching parameters λ_i , as the following examples show.

B. Crosstalk oscillations

A rather clear example of hidden oscillations was noted by Guglielmi and Hairer in [8], where their significance for numerical simulation was highlighted. They also have significance if they affect a larger discontinuous system (i.e. a system with more dimensions), as we will show. Consider the planar piecewise-constant system

$$(\dot{x}_1, \dot{x}_2) = \left(\lambda_2 - \lambda_1 + \lambda_1 \lambda_2, 3\left(\frac{1}{2}\lambda_2 - 2\lambda_1 + \lambda_1 \lambda_2\right) \right), \quad (20)$$

with $\lambda_1 = \text{sign}(x_1)$, $\lambda_2 = \text{sign}(x_2)$. The origin is a simple attractor in (x_1, x_2) space. Solutions spiral around, crossing through the switching surfaces until they reach the half-line $\{x_1 = 0 > x_2\}$, then slide in towards the intersection. Solutions to the sliding problem (6) exist only on the half-line $\{x_1 = 0 > x_2\}$, where the switching layer system is $(\lambda'_1, \dot{x}_2) = \left(-1 - 2\lambda_1, -3\left(\frac{1}{2} + 3\lambda_1\right)\right)$, giving sliding modes with $\lambda_1 = -1/2$, $\dot{x}_2 = 3$.

The switching layer system the intersection is rather more interesting, given by substituting (20) into (11) with $r = 2$,

$$(\lambda'_1, \lambda'_2) = \left(\lambda_2 - \lambda_1 + \lambda_1 \lambda_2, 3\left(\frac{1}{2}\lambda_2 - 2\lambda_1 + \lambda_1 \lambda_2\right) \right), \quad (21)$$

We make the relative timescales explicit using (12), so

$$\lambda'_1 = \varepsilon_1 \dot{\lambda}_1, \quad \lambda'_2 = \varepsilon_2 \dot{\lambda}_2,$$

for infinitesimal positive ε_1 and ε_2 . The combined phase portraits are shown in figure 3, and differ qualitatively for different values of ε_1 and ε_2 , showing a focal attractor in (i), a focal repeller in (ii) and a nodal repeller in (iii); in the repelling cases inspection of the flow reveals the existence of a limit cycle as illustrated, and we will confirm its existence with simulations below.

The switching layer system has an equilibrium at $(\lambda_1 \lambda_2) = (0, 0)$, where the jacobian (16) evaluates as

$$\begin{pmatrix} \frac{\partial \lambda'_1}{\partial \lambda_1} & \frac{\partial \lambda'_1}{\partial \lambda_2} \\ \frac{\partial \lambda'_2}{\partial \lambda_1} & \frac{\partial \lambda'_2}{\partial \lambda_2} \end{pmatrix} = \begin{pmatrix} -\varepsilon_1^{-1} & \varepsilon_1^{-1} \\ -6\varepsilon_2^{-1} & \frac{3}{2}\varepsilon_2^{-1} \end{pmatrix}$$

with determinant $9/2\varepsilon_1\varepsilon_2 > 0$ implying that the equilibrium is a focus or node, and trace $\frac{3}{2}\varepsilon_2^{-1} - \varepsilon_1^{-1}$ implying the origin is attracting for $\varepsilon_2/\varepsilon_1 > 3/2$, repelling otherwise, with a Hopf bifurcation when

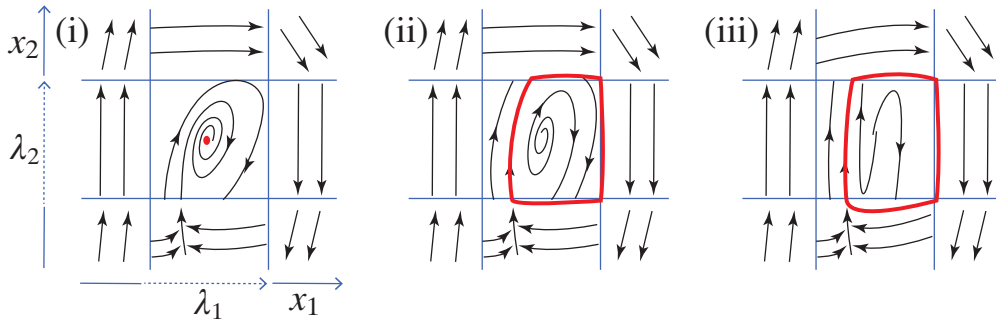


FIG. 3: Sketch of the piecewise smooth system, including the switching layers, where $\{\varepsilon_1, \varepsilon_2\}$ are: (i) $\{0.02, 0.04\}$, (ii) $\{0.02, 0.02\}$, (iii) $\{0.08, 0.02\}$.

$\varepsilon_2/\varepsilon_1 = 3/2$. The Hopf bifurcation is supercritical, creating the attracting limit cycle as shown in figure 3, wrapping partly around the boundary of the switching layer.

This cycle is bounded to the interior and edges of the switching layer $\lambda_{1,2} \in (-1, +1)$, inhabiting the intersection where the variables x_1 and x_2 are fixed at zero, so it may seem that these oscillations are of little practical consequence. This is false, however, and we will illustrate two simple ways that such oscillations can significantly impact a system.

Consider the planar system (20) to be coupled to a third variable whose dynamics involves the switching parameters λ_1 or λ_2 in some way, for example

$$\dot{x}_3 = \mu(\lambda_1 - x_3). \quad (22)$$

If the positive constant μ is large enough then x_3 tracks the value of λ_1 very closely, and the hidden oscillations become visible. Figure 4 (bold curve) shows a simulation of the value of $\lambda_1(t)$, which $x_3(t)$ attempts to track, collapsing to a steady state in (i), and forming oscillations in (ii) and (iii). These oscillations are infinitely fast (they occur on the timescale $t/\varepsilon_{1,2}$ where $\varepsilon_{1,2}$ are infinitesimal), so they are shown as a band of values (the shaded rectangle) in figure 3.

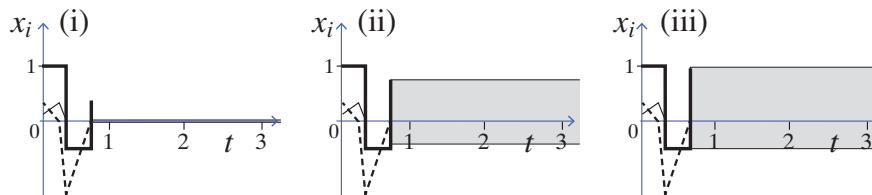


FIG. 4: Coupling of (20) to a third variable can make hidden oscillations observable. The value of $\lambda_1(t)$ is simulated here with (i)-(iii) corresponding to figure 3. The bold curve is $\lambda_1(t)$, which at $t \approx 0.8$ starts oscillating infinitely fast in the region shaded. The dashed curve shows $x_2(t)$ which settles to zero at $t \approx 0.8$, and the thin curve shows $x_1(t)$ which settles to zero at $t \approx 0.4$.

The value of $x_3(t)$ will average over these oscillations, and the precise value it takes will depend on the precise form of (22), as well as the absolute size of the constants $\varepsilon_{1,2}$, which in applications are likely to represent small rather than infinitesimal constants. This is the case if we simulate the system above by smoothing the discontinuity, which we consider now.

The consequences of the hidden oscillations for simulations performed by smoothing the discontinuity into a steep but smooth switch were highlighted in [8]. The oscillations are immediately brought to life. If we approximate the discontinuous system by replacing each $\lambda_i = \text{sign}(x_i)$ with a steep sigmoid function, say $\lambda_i = \tanh(x_i/\varepsilon_i)$, the limit cycles become cycles of order ε_i in their respective directions (which is weaker than confining them strictly to the regions $|x_i| < \varepsilon_i$). The simulations in figure 5 show, in fact, the limit cycles reaching as far as $|x_2| = 4\varepsilon_i$, creating significant and observable oscillations. In (i) a trajectory crosses through $x_2 = 0$ before hitting $x_1 = 0$,

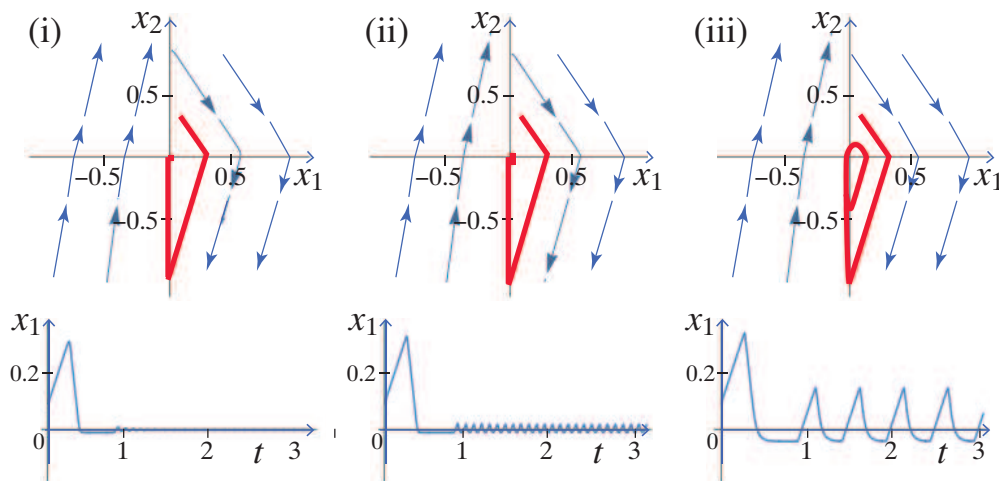


FIG. 5: Smoothing of (20) can make hidden oscillations observable. Simulations are shown in the (x_1, x_2) plane (top) and plotting $x_1(t)$ (bottom), with (i)-(iii) corresponding to figure 3.

sliding towards the intersection, and then reaching a fixed point as implied by the switching layer dynamics above. In (ii) and (iii) the intersection is repelling and creates an oscillation, which is larger in (iii) when the switching layer is nodally, rather than focally, repelling.

C. Hidden Lorenz attractor

In the same vein as the previous example, a model with hidden oscillations at an intersection of three switches was reported in [21],

$$\begin{aligned}\frac{d}{dt}x_1 &= 5(\lambda_2 - \lambda_1) - 75x_1, \\ \frac{d}{dt}x_2 &= -\lambda_1 - 15\lambda_1\lambda_3 - \frac{1}{2}\lambda_2 - 75x_2, \\ \frac{d}{dt}x_3 &= 15\lambda_1\lambda_2 - \frac{4}{3} - \frac{4}{3}\lambda_3 - 75x_3,\end{aligned}\tag{23}$$

where $\lambda_j = \text{sign}(x_j)$ for $j = 1, 2, 3$. This model is inspired by gene regulatory networks [21], where the switches are Hill functions $Z_j = \frac{1}{2} + \frac{1}{2}\lambda_j$ where threshold gene concentrations $y_j = x_j + \frac{1}{4}$ cross threshold values $y_j = \frac{1}{4}$. The triple intersection point $x_1 = x_2 = x_3 = 0$ is a simple nodal attractor in (x_1, x_2, x_3) space, so the system appears trivial, as illustrated in figure 6(i).

The dynamics on each individual surface $x_1 = 0$, $x_2 = 0$, $x_3 = 0$, found by seeking sliding modes using (6) applied separately to λ_1 , λ_2 , and λ_3 , is not particularly interesting. At their intersection, however, applying (11) with $r = 3$ to (23), we obtain the switching layer dynamics

$$\begin{aligned}\lambda'_1 &= 5(\lambda_2 - \lambda_1), \\ \lambda'_2 &= -\lambda_1 - 15\lambda_1\lambda_3 - \frac{1}{2}\lambda_2, \\ \lambda'_3 &= 15\lambda_1\lambda_2 - \frac{4}{3} - \frac{4}{3}\lambda_3,\end{aligned}\tag{24}$$

on $x_1 = x_2 = x_3 = 0$. By construction (and as was shown in [21] by singular perturbation analysis, whose relation to our switching layer analysis is described in [13]), if we assume the three primed timescale are the same ($\varepsilon_1 = \varepsilon_2 = \varepsilon_3$ in (12)) then this has a Lorenz attractor inside $\lambda_1, \lambda_2, \lambda_3 \in (-1, +1)$. So while each x_i is attracted to the intersection point and then remains fixed, the switching parameters λ_i enter into chaos.

Similar to the previous example, the chaos in the switching parameters is not directly observable through the variables $x_{1,2,3}$, which are attracted to the origin and then remain there. The implications of oscillating λ_i values may be interesting to consider in specific applications, but they become more apparent if the three dimensional system is coupled to a fourth (or fifth, etc.) variable. Then the effects of this chaos may be readily observable, for example adding

$$\dot{x}_4 = \mu(\lambda_1 - x_4),\tag{25}$$

for a sufficiently large constant μ , the variable x_4 will track the chaotic value λ_1 while the variables $x_1 = x_2 = x_3 = 0$ remain fixed. The solution for x_4 coupled with (23) is simulated in figure 7, and exhibits chaotic spiking behaviour while x_1, x_2, x_3 , remain at zero.

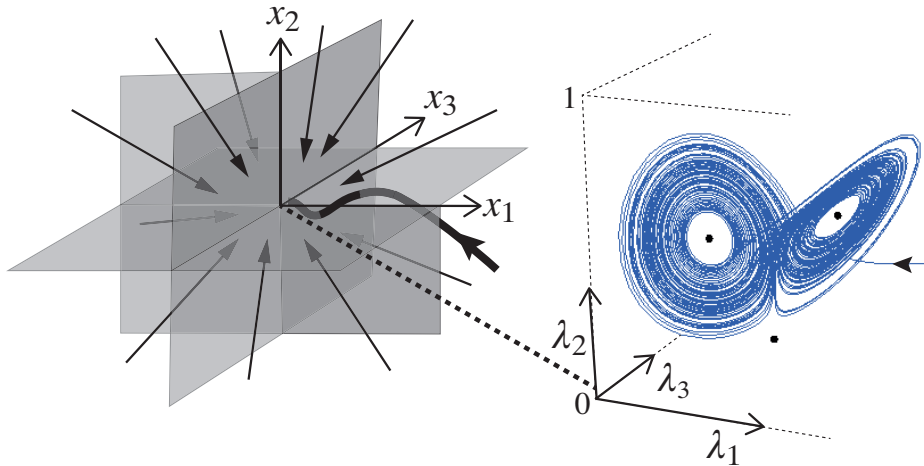


FIG. 6: Global attractor in x_1, x_2, x_3 space, and a Lorenz attractor in the switching layer inside $(x_1, x_2, x_3) = (\theta_1, \theta_2, \theta_3)$.

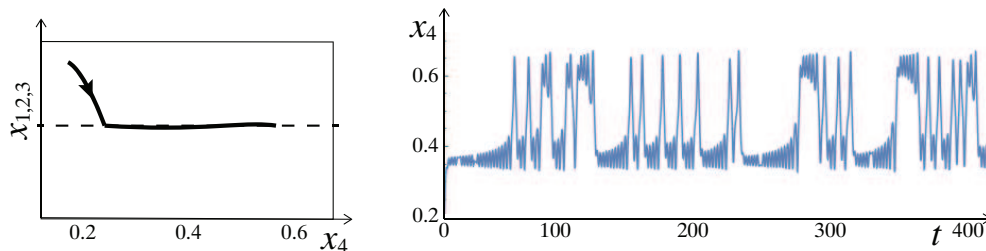


FIG. 7: Hidden chaos made visible: the dynamics of the system (23) with (25), showing a representation of the dynamics in (x_1, x_2, x_3, x_4) space where the trajectory collapses onto the line $\{x_1 = x_2 = x_3 = 0, x_4 \in \mathbb{R}\}$, and a simulation of the chaotic solution $x_4(t)$ for $\mu = 1$.

The three examples above demonstrate that hidden attractors of switching can take almost any of the interesting forms known in nonlinear dynamics, induced by any number of switches. Rather than suggest a general classification, we have therefore highlighted the ease with which they arise, and the ways they may be recognised in observations of physical data or in spurious behaviour of simulations. The last two examples were inspired by mathematical biology of gene regulatory networks, but given the ease with which they appear, these and countless other examples may have a significant role in physical and biological switching processes.

The next section moves on to systems where we show that hidden terms are required to remove degeneracies in simple scenarios that appear in the standard classifications of piecewise smooth systems.

IV. HIDDEN BIFURCATIONS

Similarly to a hidden attractor of switching, we can define a *hidden bifurcation* (of switching) as a local or global bifurcation in a dynamical system, where the bifurcating object lies at least partly inside the switching surface, and whose existence is not apparent from an inspection of the vector fields outside the switching surface.

Bifurcations of basic singularities of planar systems, particularly of equilibria hitting the switching surface (*boundary equilibrium bifurcations*), or of tangencies between a vector field and the switching surface, have been a key point of interest in recent piecewise smooth systems theory, e.g. in [1, 5, 6, 18]. We revisit two elementary cases here that have the quirk that the attractivity of an equilibrium flips in an unexplained way, and we reveal the hitherto unconsidered role of hidden dynamics in such bifurcations. We consider one boundary equilibrium bifurcation and one tangency bifurcation, both in a planar system with a single switch. Lastly we show a hidden bifurcation in two dimensions that determines the passibility or not of a switching threshold.

A. The flipping node

Consider the planar system

$$(\dot{x}_1, \dot{x}_2) = \frac{1+\lambda}{2}(x_1 + 2x_2 - \alpha, x_2) + \frac{1-\lambda}{2}(1, 3), \quad (26)$$

where $\lambda = \text{sign}(x_1)$ for $x_1 \neq 0$, and α is a bifurcation parameter. For $\alpha \geq 0$ this system has a repelling node at $x_1 = \alpha$, $x_2 = 0$. As we decrease α through zero the node hits the switching surface. From the arrangements of the vector fields it is simple to sketch the phase portrait, shown in figure 8. (This was studied recently in [10], the singularity at $\alpha = 0$ having been given in [5], and the omission of this case from more recent classifications of boundary equilibrium bifurcations such as [1, 6, 18] highlights the subtle difficulty of qualitative nonsmooth dynamics).

Analysing the switching layer dynamics by substituting (26) into (5), we find that there is a sliding manifold \mathcal{M}^S as defined in (7), given by $(\lambda, x_2) \in (-1, +1) \times \mathbb{R}$ such that $\lambda = \frac{1+2x_2-\alpha}{1-2x_2+\alpha}$, which exist for $x_2 < \alpha/2$ (ensuring $\lambda \in (-1, +1)$). Substituting λ into (27) gives the sliding dynamics $\dot{x}_2 = \frac{3\alpha-5x_2}{1-2x_2+\alpha}$, $x_1 = 0$. The denominator of \dot{x}_2 is positive since $x_2 < \alpha/2 < (1+\alpha)/2$, then the numerator implies that there exists an attractor (a *psuedoequilibrium*) in the sliding dynamics at $x_2^* = 3\alpha/5$, and since this can exist only for $x_2^* = 3\alpha/5 < \alpha/2$, the sliding equilibrium exists only for $\alpha < 0$.

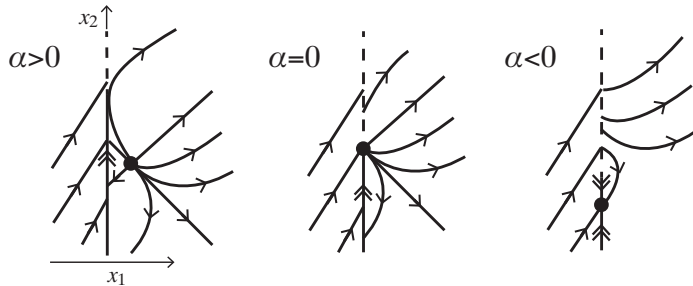


FIG. 8: As α changes sign, a repelling node hits the switching surface, and becomes an attracting (equilibrium-) node in the sliding dynamics.

This seems to complete the picture of this simple bifurcation. There is one fixed point in the system, given for $\alpha > 0$ by a repelling node in $x_1 > 0$, which approaches the switching surface as α changes sign, and becomes for $\alpha < 0$ an attracting node on $x_1 = 0$ in the region $x_2 < 0$.

The curiosity of this *boundary equilibrium bifurcation* is that the attractivity of the node flips during the bifurcation. To see how this happens requires closer inspection of the dynamics on $x_1 = 0$.

The switching layer system, given by substituting (26) into (5), is

$$(\lambda', \dot{x}_2) = \frac{1+\lambda}{2}(2x_2 - \alpha, x_2) + \frac{1-\lambda}{2}(1, 3) \quad \text{on } x_1 = 0, \quad (27)$$

which has an equilibrium at $\lambda^* = (5+\alpha)/(5-\alpha)$ with $x_2^* = 3\alpha/5$, corresponding to the equilibrium found above for $\alpha < 0$. This means we can understand the node as entering the switching layer at $\lambda = +1$ when α becomes negative. Introducing the infinitesimal ε by (12), the jacobian (16) (for $r = 1$) at this equilibrium is

$$\begin{pmatrix} \frac{\partial \lambda'}{\partial \lambda} & \frac{\partial \lambda'}{\partial x_2} \\ \frac{\partial \dot{x}_2}{\partial \lambda} & \frac{\partial \dot{x}_2}{\partial x_2} \end{pmatrix} = \frac{1}{2\varepsilon} \begin{pmatrix} \frac{\alpha}{5} - 1 & \frac{4}{1-\frac{\alpha}{5}} \\ 3(\frac{\alpha}{5} - 1)\varepsilon & \frac{2}{1-\frac{\alpha}{5}}\varepsilon \end{pmatrix},$$

with determinant and trace

$$\det = \frac{5}{2\varepsilon}, \quad \text{tr} = \frac{1}{2\varepsilon} \left\{ 2\varepsilon - \left(\frac{\alpha}{5} - 1 \right)^2 \right\} / \left(1 - \frac{\alpha}{5} \right).$$

These reveal that the equilibrium is an attractor for $\alpha < 5(1 - \sqrt{2\varepsilon})$, hence for small α (with small ε by definition) it is always an attractor. For small α and ε , specifically for $(11 - 2\sqrt{30})(\alpha - 5)^2 - 50\varepsilon > 0$ (e.g. for $\forall \alpha$ if $\varepsilon = 0$, for $\varepsilon < 1/2(11 + 2\sqrt{30}) \approx 0.023$ if $\alpha = 0$) the eigenvalues are real, indicating a node.

Thus at $\alpha = 0$ we have a matching of two opposing systems describing the node at $x_1 = x_2 = 0$, that of a repelling node outside the switching layer, and an attracting node inside the layer, yielding

the phase portraits in figure 9. We can describe this as a *folded node*, the stitching together of phase portraits of nodes that are attracting and repelling on different halves of the plane. The figure reveals that when $\alpha = 0$, there exist a whole family of cycles through the folded singularity, in the region bounded by \mathcal{M}^S and the strong unstable manifold of the repelling node (labelled \mathcal{U}).

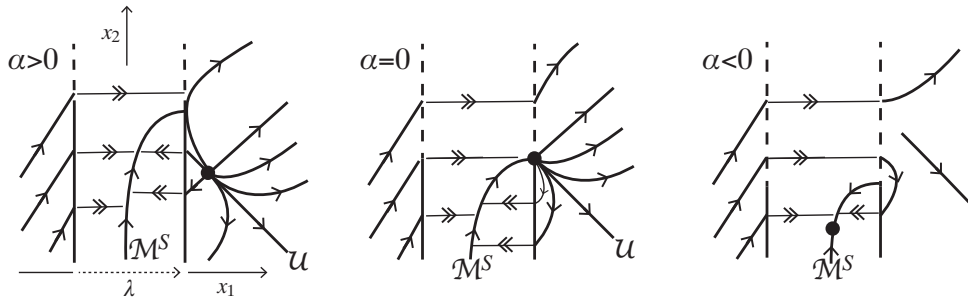


FIG. 9: The bifurcation in figure 8 with the switching surface $x_1 = 0$ blown up into a layer $\lambda \in (-1, +1)$.

This gives more insight into the phase portrait at $\alpha = 0$, but reveals that the $\alpha = 0$ system is degenerate, in the sense that it contains a folded node on the boundary of the switching layer $\lambda = +1$, associated with an infinite family of closed cycles. The degeneracy is not broken by adding functions of x_1 or x_2 to (26), but it can be broken by adding a term nonlinear in λ . A simple perturbation of (26), say

$$(\dot{x}_1, \dot{x}_2) = \frac{1+\lambda}{2} (x_1 + 2x_2 - \alpha, x_2) + \frac{1-\lambda}{2} (1, 3) + (\lambda^2 - 1) (\beta, 0), \quad (28)$$

will be sufficient, with $\beta > 1/4$. In this system, the degeneracy that occurred at $\alpha = 0$ is broken, and revealed as a Hopf bifurcation. We show this as follows.

The system outside $x_1 = 0$ is unchanged because β affects only the switching layer, where $\lambda \in (-1, +1)$. The equilibrium in the switching layer for this perturbed system lies at $\lambda^* = \frac{1}{4\beta} (\alpha - 5 - R)$, $x_2^* = \frac{3}{10} (\alpha + 5 + 4\beta + R)$, where $R = \sqrt{(\alpha - 5)^2 + 8\beta(\alpha + 5 + 2\beta)}$, and the associated jacobian (16) becomes

$$\begin{pmatrix} \frac{\partial \dot{\lambda}}{\partial \lambda} & \frac{\partial \dot{\lambda}}{\partial x_2} \\ \frac{\partial \dot{x}_2}{\partial \lambda} & \frac{\partial \dot{x}_2}{\partial x_2} \end{pmatrix} = \frac{1}{2\varepsilon} \begin{pmatrix} \frac{1}{5} (3(\alpha - 5) + 12\beta + 2R) & 2(1 + \frac{1}{4\beta} (\alpha - 5 + R)) \\ \frac{3}{10} (r - R) \varepsilon & (1 + \frac{1}{4\beta} (\alpha - 5 + R)) \varepsilon \end{pmatrix}$$

where $r = \alpha - 5 + 4\beta$. Its trace is $tr = \frac{1}{10} (3(\alpha - 5) + 12\beta + 2R) + \frac{\varepsilon}{2} (1 + \frac{1}{4\beta} (\alpha - 5 + R))$, which in the $\varepsilon \rightarrow 0$ limit becomes $\frac{1}{10} (3(\alpha - 5) + 12\beta + 2R)$. Most importantly, at the bifurcation this is $tr = \frac{1}{2} (4\beta - 1)$, which is positive for $\beta > 1/4$, hence at the bifurcation the equilibrium is now a simple repelling node, and the degeneracy is broken, the point $x_1 = x_2 = 0$ now being a repelling node both inside and outside the switching layer.

The flip in attractivity of the node now occurs via a Hopf bifurcation inside the switching layer, occurring when the trace vanishes, $0 = tr = \frac{1}{10} (3(\alpha - 5) + 12\beta + 2R) + \frac{\varepsilon}{2} (1 + \frac{1}{4\beta} (\alpha - 5 + R)) = \frac{1}{10} (3(\alpha - 5) + 12\beta + 2R) + \mathcal{O}(\varepsilon)$, at an α value

$$\alpha_h = \alpha_{h0} - 3\varepsilon/\sqrt{\beta} + \mathcal{O}(\varepsilon^2) , \quad \text{where} \quad \alpha_{h0} = 5 - 8\sqrt{\beta} - 4\beta . \quad (29)$$

Prior to this, as α decreases from zero, the equilibrium changes from a node into a focus, when the eigenvalues of the jacobian change from real to complex, at $0 = 8\beta^2 r^2 + 40\beta(8\beta - 5\varepsilon)^2 - 9600\beta^2\varepsilon + (8\beta - 5\varepsilon)(12\beta - 5\varepsilon)(r + R)r = 8\beta^2 r^2 + 40\beta(8\beta - 5\varepsilon)^2 - 9600\beta^2\varepsilon + (8\beta - 5\varepsilon)(12\beta - 5\varepsilon)(r + R)r + \mathcal{O}(\varepsilon^2)$, at an α value

$$\alpha_f = \alpha_{h0} \pm 12\sqrt{3\varepsilon} + \mathcal{O}(\varepsilon) . \quad (30)$$

The resulting phase portrait is shown in figure 10.

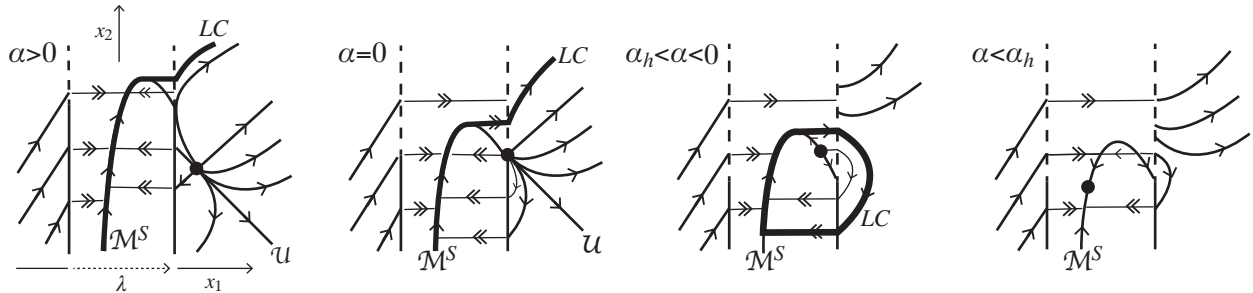


FIG. 10: The bifurcation in the perturbed system as α passes through $\alpha = 0$ and α_h . A limit cycle labelled LC in (ii-iii), shrinks until a supercritical Hopf bifurcation occurs, giving the change in the equilibrium's attractivity from (iii) to (iv).

The bifurcation is split into stages, by means of which the node is able to change from repelling for $\alpha > 0$ to attracting for $\alpha < 0$, and we will describe these qualitatively.

There first exists the repelling node outside the switching layer (shown in the first picture), and all trajectories in the system evolve towards infinity. The continuation of the sliding manifold M^S forms an orbit, labelled LC and shown in bold, which will be important in the subsequent bifurcation.

At $\alpha = 0$ the node touches the boundary layer, but otherwise the phase portrait is not critically different from $\alpha > 0$. At $\alpha = \alpha_f$ (not shown) this node becomes a repelling focus, resulting (since $0 < \alpha_f < \alpha_h$) in the third picture in figure 10 for $\alpha < \alpha_f$. At some $0 < \alpha < \alpha_h$ between the second and third pictures, the trajectory LC emitted from M^S intersects the strong manifold of

the vanished equilibrium of the $x_1 > 0$ system (labelled \mathcal{U}), after which LC is seen to form an attracting limit cycle surrounding the focus.

At $\alpha = \alpha_h$ the limit cycle shrinks to zero and thus the focus's attractivity changes in a supercritical Hopf bifurcation, giving the far right picture in figure 10. At some further $\alpha = \alpha_f < \alpha_h$, not shown, the equilibrium will become a node again, now attracting.

These features, particularly the existence of the limit cycle, are implied by the local phase portrait. To prove these steps rigorously requires matching the different flows outside the layer with those inside the layer on and off of \mathcal{M}^S . We omit such lengthy analysis here, but support and illustrate the results with simulations as follows.

We simulate an approximation of (28) in which the discontinuity is replaced by a steep sigmoid function, replacing $\lambda = \text{sign}(x_1)$ with $\lambda = \tanh(x_1/\varepsilon)$ with $\varepsilon = 10^{-3}$. Singular perturbation analysis of piecewise smooth systems [22, 25] imply that such a system should approximate the dynamics found in the switching layer analysis above. The resulting flows are shown in figure 11, for α values corresponding to those in figure 10. The x_1 scale is stretched inside the region $|x_1| < \varepsilon$, which is analogous to blowing up the switching layer, to reveal the Hopf bifurcation in the switching layer.

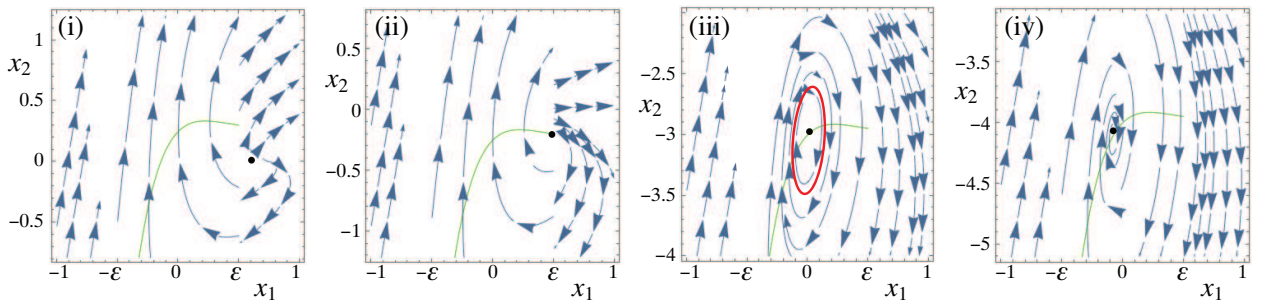


FIG. 11: Simulation of a smoothing of (28) with $\beta = 1/2$, at α values (i) 0.5, (ii) 0, (iii) -6 , (iv) -8 . The thin curve in all four pictures is the set $\lambda' = 0$, which approximates the sliding manifold \mathcal{M}^S in the limit $\varepsilon \rightarrow 0$ and where it is not close to horizontal. The limit cycle in (iii) is shown.

The flow exhibits the qualitative behaviour predicted above, namely that a repelling node enters the switching layer (now $|x_1| < \varepsilon$) at $\alpha = 0$, becomes a repelling focus surrounded by an attracting limit cycle, which is annihilated in a Hopf bifurcation as the focus changes stability.

Clearly this bifurcation is interesting in itself and warrants more detailed analysis, but we shall leave deeper study to future work, having shown the role of hidden terms in breaking the degeneracy. We shall now compare this to one other case of flipping attractivity, this time induced

by a bifurcation of tangencies and resulting in a more obvious degeneracy, and will see the the resolution is similar in principle.

B. The flipping pseudonode

Proceeding along similar lines to the last section, consider the system

$$(\dot{x}_1, \dot{x}_2) = \frac{1+\lambda}{2} (x_2 - 2\alpha, 2 + \hat{\beta}x_2) - \frac{1-\lambda}{2} (x_2, 1) + (\lambda^2 - 1)(\beta, 0), \quad (31)$$

where α is a bifurcation parameter and $\beta, \hat{\beta}$, are constants. In this section we introduce perturbations β and $\hat{\beta}$ from the outset. The phase portrait with $\beta = \hat{\beta} = 0$, shown in figure 12, appears at first to unfold a simple bifurcation in which the relative position of two tangencies along the switching surface is exchanged. (For more details of this with $\beta = \hat{\beta} = 0$ see [18]).

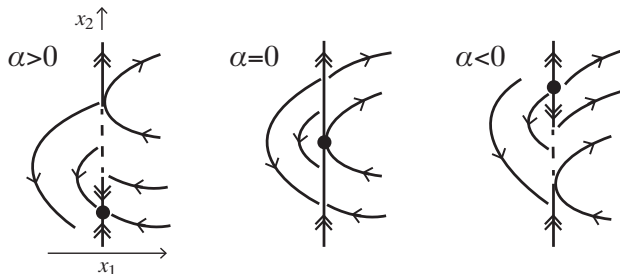


FIG. 12: A bifurcation in which visible ('curving away from $x_1 = 0$ ') and invisible ('curving towards $x_1 = 0$ ') folds in the flow exchange ordering, is accompanied by a (pseudo)-node changing from attracting to repelling.

The switching layer system, given by substituting (31) into (5), is

$$(\lambda', \dot{x}_2) = \frac{1+\lambda}{2} (x_2 - 2\alpha, 2 + \hat{\beta}x_2) - \frac{1-\lambda}{2} (x_2, 1) + (\lambda^2 - 1)(\beta, 0) \quad \text{on } x_1 = 0. \quad (32)$$

Neglecting β to begin with, the switching surface is attracting for $x_2 < \min(0, 2\alpha)$ and repelling for $x_2 > \max(0, 2\alpha)$ (for small β these boundaries change only slightly). Sliding modes exist where $\lambda = \alpha/(x_2 - \alpha)$ for $|\alpha/(x_2 - \alpha)| < 1$, and their dynamics is given by $\dot{x}_2 = \frac{x_2 + 2\alpha}{2(x_2 - \alpha)}$. The sliding system itself has a node type equilibrium where (32) vanishes, at $x_2^* = -2\alpha$, $\lambda^* = -1/3$. Near this equilibrium we can expand $\dot{x}_2 = -(x_2 + 2\alpha)/6\alpha + \mathcal{O}((x_2 + 2\alpha)^2)$, implying that the node is attracting for $\alpha > 0$ and repelling for $\alpha < 0$.

So as α changes from positive to negative with $\beta = \hat{\beta} = 0$, an attracting node in negative x_2 moves to become a repelling node in positive x_2 , as sketched in figure 13. We omit the calculations for $\beta = \hat{\beta} = 0$ because, as in the previous section, some explanation is now required for how the flip in attractivity occurs.

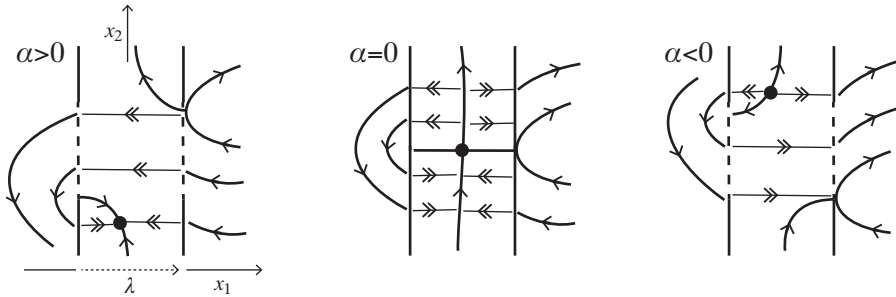


FIG. 13: The bifurcation in figure 12, with $x_1 = 0$ blown up into the layer $\lambda \in (-1, +1)$.

For $\beta = \hat{\beta} = 0$, the switching layer system (32) actually contains two topological degeneracies which coincide with the flip in the node's attractivity, firstly because (32) becomes a centre when $\alpha = 0$, and secondly because the nullcline $\lambda' = 0$ has segments lying parallel to the fast (λ) direction when $\alpha = 0$, the latter of which illustrated in figure 13. The first of these is broken by taking $\hat{\beta} \neq 0$, as is easily verified by simulation of the switching layer system. The Sotomayor-Teixeira regularization [25] of such a system is studied in [17] using singular perturbation methods, but this does not break the second degeneracy, which indeed can only be broken by taking $\beta \neq 0$ (see [13] for a general study of this degeneracy). We will set $\hat{\beta}$ to zero, since $\beta \neq 0$ is sufficient to break both degeneracies.

Sliding modes, found by applying (6) to (31), are given by solving $\lambda' = 0$ in (32), and thus satisfy $\beta\lambda^2 + (x_2 - \alpha)\lambda - \beta - \alpha = 0$, with solutions $\lambda = \frac{\alpha - x_2}{2\beta} \pm \sqrt{\frac{(\alpha - x_2)^2}{4\beta^2} + 1 + \frac{\alpha}{\beta}}$, and $|\lambda| < 1$ then implies that sliding modes exist for $(x_2 - \alpha)^2 > -4\beta^2(1 + \frac{\alpha}{\beta})$. The switching layer equilibrium lies at $\lambda^* = -1/3$, $x_2^* = -2\alpha - 8\beta/3$, with jacobian

$$\begin{pmatrix} \frac{\partial \lambda}{\partial \lambda} & \frac{\partial \lambda}{\partial x_2} \\ \frac{\partial \dot{x}_2}{\partial \lambda} & \frac{\partial \dot{x}_2}{\partial x_2} \end{pmatrix} = \frac{1}{\varepsilon} \begin{pmatrix} \frac{10}{3}\beta - 3\alpha & -\frac{1}{3} \\ \frac{3}{2}\varepsilon & 0 \end{pmatrix},$$

whose trace changes sign at $\alpha = \alpha_h := -\frac{10}{9}\beta$, suggesting that a Hopf bifurcation occurs in the switching layer system, facilitating the change in attractivity of the equilibrium.

The perturbation has two important consequences. First, when $\alpha = 0$ the trace of the jacobian is $-\frac{10}{3}\beta$ so the equilibrium is non-degenerate, and secondly, when the supposed Hopf bifurcation occurs at $\alpha = \alpha_h$, the switching layer system is given by

$$(\lambda', \dot{x}_2) = \frac{1 + \lambda}{2} (x_2 - 2\alpha_h, 2) - \frac{1 - \lambda}{2} (x_2, 1) + (\lambda^2 - 1)(\beta, 0),$$

which is not a centre. As a result, for $\beta \neq 0$, a non-degenerate Hopf bifurcation takes place at $\alpha = \alpha_h = -\frac{10}{9}\beta$, which lies on one side or the other of the bifurcation of tangencies which occurs at $\alpha = 0$, depending on the sign of β .

The switching layer is shown in figure 14. By varying α , with β either negative or positive, we obtain the sequences of bifurcations described qualitatively as follows.

First we take negative β , shown in the top row of figure 14. For α positive and greater than α_h we begin with an attracting equilibrium inside the switching layer, which undergoes a supercritical Hopf bifurcation at $\alpha = \alpha_h$, becoming a repelling equilibrium surrounded by an attracting limit cycle which grows as α decreases; these steps form the first three pictures. The cycle is formed by the continuation of the sliding manifold \mathcal{M}^S under the flow. During these changes no bifurcation is evident in the vector field outside the switching layer, and the repelling equilibrium and cycle are a hidden repeller/attractor respectively. As α continues to decrease, the two branches of the sliding manifold \mathcal{M}^S bifurcate to form the arrangement in the last picture, the repelling equilibrium passes from one branch to the other in the process, and the limit cycle formed by the continuation of \mathcal{M}^S tails off to infinity. As α passes through zero where the two tangencies exchange ordering along the switching surface, no further qualitative changes occur inside the switching layer.

The process for positive β is slightly different, shown in the bottom row of figure 14. For α positive and greater than α_h we again have an attracting equilibrium inside the switching layer. The continuation of the sliding manifold \mathcal{M}^S under the flow is highlighted as a bold curve, which is important in the bifurcation. As α passes through zero, the tangencies exchange ordering along the switching surface, the two branches of \mathcal{M}^S bifurcate, the attracting equilibrium moves from one branch to the other, and the continuation of \mathcal{M}^S forms a limit cycle, shown in the second picture. The equilibrium and the cycle are a hidden attractor/repeller respectively, and from the vector field outside the switching surface the equilibrium appears to be repelling. In fact the equilibrium only becomes repelling after a subcritical Hopf bifurcation at $\alpha = \alpha_h$ in the third picture, leaving a repelling equilibrium on the repelling branch of the sliding manifold \mathcal{M}^S , as in the fourth picture.

As in the last section, we conclude by simulating the system (31) by smoothing out the discontinuity, replacing $\lambda = \text{sign}(x_1)$ with $\lambda = \tanh(x_1/\varepsilon)$ and $\varepsilon = 10^{-3}$. Similar to figure 11 we stretch the x_1 axis for $|x_1| < \varepsilon$, to blow up the switching layer and reveal its hidden dynamics. In figure 15, simulations are shown which correspond to the bottom row of figure 14 with $\beta > 0$, showing a focus changing stability via a subcritical Hopf bifurcation which take place at negative α , after the bifurcation of tangencies has occurred at $\alpha = 0$.

Similar results can be achieved to resolve other bifurcations and degeneracies. The cases above merit deeper study, as do similar bifurcations found in [1, 5, 6, 18], but to achieve a level of generality it will be necessary to develop the notion of normal forms and topological equivalences

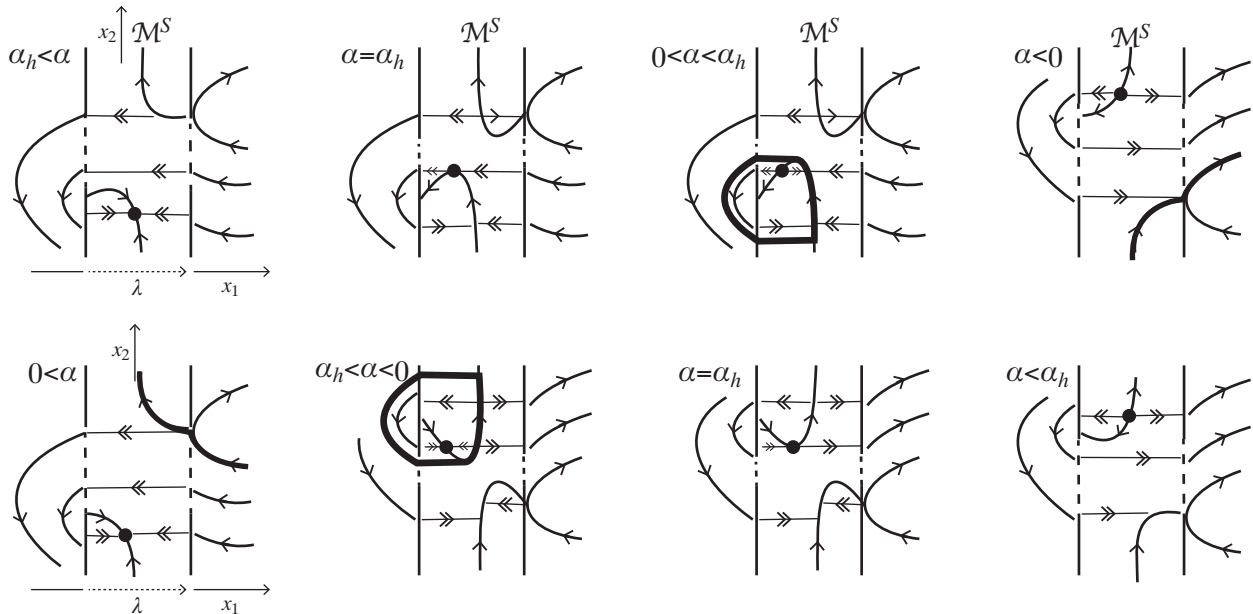


FIG. 14: The bifurcation for $\beta < 0$ (implying $\alpha_h > 0$) is shown in the top row, giving a supercritical Hopf bifurcation; the case for $\beta > 0$ (implying $\alpha_h < 0$) is shown in the bottom row, giving a subcritical Hopf bifurcation.

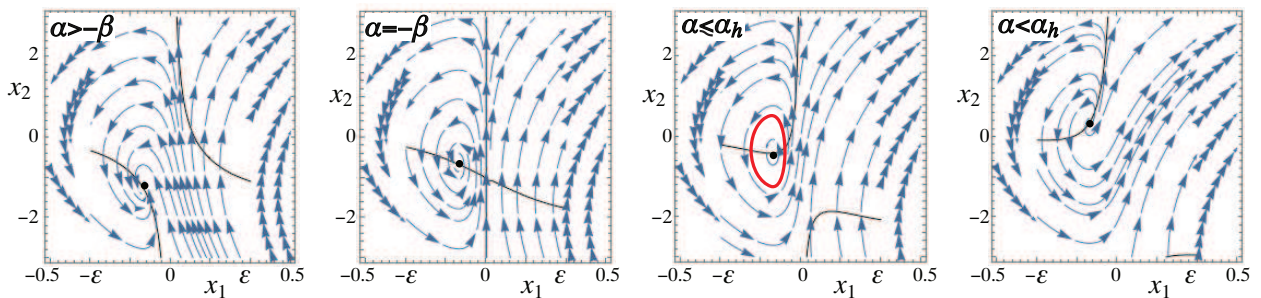


FIG. 15: Simulation of the subcritical case. Between the second and third panels, a repelling limit cycle is seen to shrink quickly from infinite size to the one show for $\alpha \lesssim \alpha_h$. The specific values are $\alpha = -7/9, -17/30, -1/2, -1/3$, respectively, with $\beta = 1/2$.

between such systems much further than has been done at present. Our hope is that highlighting examples like those above will help stimulate work in this direction.

The effect of hidden terms in bifurcations can be much simpler and less subtle than in the examples above, as in the next example involving a planar system with two switches.

C. Saddle-node at a switching intersection

When multiple switches occur on different surfaces $h_1 = 0$, $h_2 = 0$, ..., $h_r = 0$, and those surfaces intersect, there may be numerous vector fields pointing into *and* out of an intersection simultaneously, and whether or not sliding occurs is less obvious than at a single switching surface, even in the absence of anomalies from nonlinear dependence on some λ_i . The piecewise smooth vector fields outside the switching surface can be deceptive, and analysis of the switching layer is vital.

Consider the system

$$\begin{aligned}\frac{d}{dt}x_1 &= \frac{1}{2}(1 - \lambda_1\lambda_2) - \gamma_1(x_1 + \theta_1) \\ \frac{d}{dt}x_2 &= \frac{1}{4}(3 - \lambda_1 - \lambda_2 - \lambda_1\lambda_2) - \gamma_2(x_2 + \theta_2)\end{aligned}\quad (33)$$

where $\lambda_i = \text{sign}(x_i)$ for some constants $\theta_1, \theta_2, \gamma_1, \gamma_2$. Nontrivial hidden dynamics in such a system enters through the multilinear dependence on the λ_i 's. This example is taken from a model of protein product concentrations x_i in a two gene regulatory system [4, 24], where the switches come in the form of Hill functions $Z_i = y_i^k / (y_i^k + \theta_i^k) \xrightarrow{k \rightarrow \infty} \frac{1}{2} + \frac{1}{2} \text{sign}(y_i - \theta_i)$, which we replace by $Z_i = \frac{1}{2} + \frac{1}{2} \lambda_i$. The phase portrait of (33) is sketched in the main picture in figure 16.

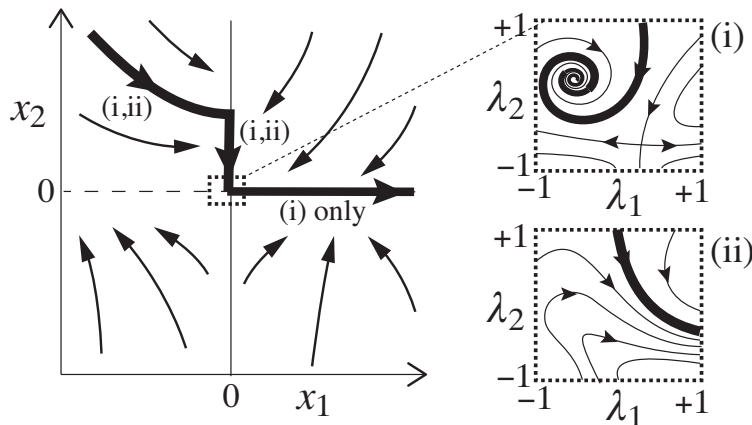


FIG. 16: Phase portrait of the fold catastrophe in the gene model, with $\theta_1 = \theta_2 = 1$, $\gamma_2 = 0.9$, and with: (i) $\gamma_1 = 0.6$, (ii) 0.4.

When $x_1 \neq 0$ and $x_2 \neq 0$, the system (33) is smooth and easily solved. We can apply the transition dynamics (11) to each of the switching thresholds $x_1 = 0$ and $x_2 = 0$ independently. We can work in terms of either λ_i or Z_i , let us choose the former. Then (5) gives the switching layer systems

$$\begin{aligned}(\lambda'_1, \dot{x}_2) &= \left(\frac{1}{2}(1 - \lambda_1\lambda_2) - \gamma_1\theta_1, \frac{1}{4}(3 - \lambda_1 - \lambda_2 - \lambda_1\lambda_2) - \gamma_2(x_2 + \theta_2) \right) \text{ on } x_1 = 0, \\ (\dot{x}_1, \lambda'_2) &= \left(\frac{1}{2}(1 - \lambda_1\lambda_2) - \gamma_1(x_1 + \theta_1), \frac{1}{4}(3 - \lambda_1 - \lambda_2 - \lambda_1\lambda_2) - \gamma_2\theta_2 \right) \text{ on } x_2 = 0.\end{aligned}\quad (34)$$

Seeking equilibria of the fast (primed) subsystems as in (6), we find that sliding modes exist on the surfaces $x_1 = 0$ with $x_2 \neq 0$, and on $x_2 = 0$ with $x_1 > 0$, elsewhere the flow crosses the switching surfaces. The flow slides towards the point where the two switches intersect at $x_1 = x_2 = 0$. (This point is reached by large regions of initial conditions but is not a global attractor). To study the switching layer inside the intersection point we apply (11) with $r = 2$, giving

$$(\lambda'_1, \lambda'_2) = \left(\frac{1}{2}(1 - \lambda_1\lambda_2) - \gamma_1\theta_1, \frac{1}{4}(3 - \lambda_1 - \lambda_2 - \lambda_1\lambda_2) - \gamma_2\theta_2\right) \text{ on } x_1 = x_2 = 0. \quad (35)$$

This is sketched in the two panels (i-ii) in figure 16. It has potentially two equilibria, a focus and a saddle at

$$\{\lambda_1^\pm, \lambda_2^\pm\} = (1 + \gamma_1\theta_1 - 2\gamma_2\theta_2) \{1, 1\} \pm \sqrt{d} \{-1, 1\}$$

where $d = (\frac{1}{2}\gamma_1\theta_1 + \gamma_2\theta_2)^2 - \gamma_1\theta_1 - \gamma_2\theta_2$, which exist only for $d > 0$, disappearing in a saddlenode bifurcation as $\{\lambda_1^\pm, \lambda_2^\pm\}$ become complex. As a result, for $d > 0$ the variables $x_{1,2}$ become fixed at the origin, while for $d < 0$ they evolve through the intersection point $(0, 0)$ and continue along $x_2 = 0$ with increasing x_1 , as shown in the main part of figure 16.

We take the opportunity here to propose a nomenclature that will be helpful in studying intersections in future work. Essentially four things can happen when a trajectory arrives at an intersection: crossing, sticking, jamming, or pausing. When a trajectory arrives at a switching surface intersection, we say it *crosses* if it passes through (either to another sliding region or to outside the switching surface), we say it *sticks* if it remains on the intersection and begins sliding along it, and we say it becomes *jammed* if no subsequent motion occurs because the trajectory has impacted at a fixed point. *Pausing* describes a trajectory that reaches a fixed point on a switching intersection in finite time, but which can be continued beyond that point after any arbitrary finite time.

Figure 17 shows local portraits that lead to three of these behaviours, generated by the following piecewise constant systems:

$$\text{crossing : } (\dot{x}_1, \dot{x}_2) = (1, 1 + \lambda_1 - \lambda_2) \quad (36)$$

$$\text{jamming : } (\dot{x}_1, \dot{x}_2) = (-\lambda_1, \frac{1}{2} + \lambda_1 - \lambda_2) \quad (37)$$

$$\text{pausing : } (\dot{x}_1, \dot{x}_2) = (-\lambda_1, \lambda_2 + \lambda_1\lambda_2) \quad (38)$$

where the named behaviour occurs at the intersection. Sticking occurs when the three trajectories shown in figure 17 reach the surface $x_1 < 0 = x_2$, and would occur at the intersection in the second example instead of jamming if we added a third equation such as $\dot{x}_3 = 1$.

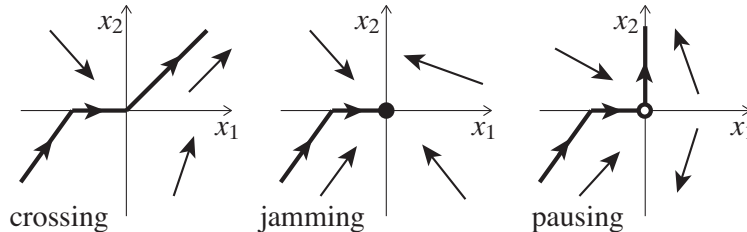


FIG. 17: The three basic possibilities when a trajectory reaches a switching intersection in finite time: crossing, jamming, or pausing.

In the example of figure 16, a bifurcation inside the switching layer of the intersection permits the system to change from jamming at the intersection to crossing through it.

The huge possibilities for the different forms of such behaviours, and their role in local and global bifurcations, are hinted at by the examples above and the three types of behaviour in figure 17. A study which uses hidden dynamics to classify the typical ways a trajectory may behave when it enters an intersection of two switches in a planar system has been made in [8]. The example above fits into the classification. For higher dimensions a full classification is generally impossible, but the possibilities for hidden bifurcations are evidently vast.

V. IN CLOSING

The study of local attractors and local bifurcations is, despite substantial classifications for planar systems in [5, 6, 8, 18], and even for three dimensional systems in [26], still subject to many unsolved problems, even in the plane. These include some lack of clarity around the definitions of equivalence classes and structural stability, and questions remain about the generality of Filippov’s usually adopted ‘convex method’ for solving at a discontinuity (noting that Filippov himself considered much more general kinds of behaviour via differential inclusions [5] and we cited some alternatives in the introduction), particularly in regard to physical applications of piecewise smooth theory [1, 7]. The successes of the schemes in these references is a reason for optimism, but evidently piecewise smooth theory is still in the early stages of addressing such problems. We hope that highlighting attractors and bifurcations of the kind analysed here will encourage deeper study of the issues they raise in regard to the dynamics that is possible at a switch and the degeneracies it can suffer.

The first example presented here, that of a van der Pol oscillator hidden inside the switching layer, is an example of phenomena exhibited only if a system has a nonlinear dependence on the

switching parameter $\lambda = \text{sign}(h)$. The two examples that followed, of limit cycles and chaotic attractors, showed that such conditions arise inescapably in systems with multilinear products $\lambda_1\lambda_2\dots$ between different switching parameters.

The examples of bifurcations given here, whose resolution requires inspection of the switching layer, were all taken from previous literature. The degeneracies we reveal inside the switching layer, however, at least for the cases with a single switch, have not been considered before.

The switching layer method is related to regularization methods, which study a smoothing of the discontinuity (as we did above for the sake of simulations only) using singular perturbation techniques, e.g. in [17, 20, 22, 27]. To-date these typically follow the Sotomayor-Teixeira [25] approach, and restrict the class of smoothed systems studied to those with strictly linear dependence on the switching parameter (i.e. with $\mathbf{g} \equiv 0$ in (3) and $\Gamma \equiv 0$ in (9)), and therefore exclude any role for the nonlinear terms used here to break degeneracies in the switching dynamics, a more general description of which can be found in [13]. It must be remembered that the interest for the discontinuous system, of course, is the limit $\varepsilon \rightarrow 0$ itself (and $\varepsilon_i \rightarrow 0$ for all i in (12)), and not, as in singular perturbation theory, what happens under perturbation to ε nonzero.

A normal form theory for the expression of local vector fields that consider the switching layer is a topic for future work, as new examples of attractors and bifurcations come to light. Our purpose here has been to provide models that show, while not being directly observable from the form of the vector fields away from the switch, nonlinear switching terms have a role in breaking degeneracy, and in creating dynamics that affects a system's dynamics.

We emphasise that the terms ‘hidden bifurcation’ and ‘hidden attractor of switching’ as described here relate to the *hidden dynamics* introduced in [8, 12], pertaining to dynamics hidden inside the switching layer of a discontinuous vector field. They are not related to Leonov’s ‘hidden attractors’ introduced in [19], which describe difficult to locate attractors whose basins of attraction do not intersect with neighbourhoods of equilibria.

Acknowledgements

MRJ’s research is supported by EPSRC Fellowship grant EP/J001317/2.

-
- [1] M. di Bernardo, C. J. Budd, A. R. Champneys, and P. Kowalczyk. *Piecewise-Smooth Dynamical Systems: Theory and Applications*. Springer, 2008.

- [2] M. di Bernardo, P. Kowalczyk, and A. Nordmark. Sliding bifurcations: a novel mechanism for the sudden onset of chaos in dry friction oscillators. *Int. J. Bif. Chaos*, 10:2935–2948, 2003.
- [3] C. Edwards and S. K. Spurgeon. *Sliding Mode Control*. Taylor & Francis, 1998.
- [4] R. Edwards, A. Machina, G. McGregor, and P. van den Driessche. A modelling framework for gene regulatory networks including transcription and translation. *Bull. Math. Biol.*, 77:953–983, 2015.
- [5] A. F. Filippov. *Differential Equations with Discontinuous Righthand Sides*. Kluwer Academic Publ. Dordrecht, 1988 (Russian 1985).
- [6] M. Guardia, T. M. Seara, and M. A. Teixeira. Generic bifurcations of low codimension of planar Filippov systems. *J. Differ. Equ.*, pages 1967–2023, 2011.
- [7] J. Guckenheimer. Review of [1] by Budd, Champneys, di Bernardo, Kowalczyk. *SIAM Review*, 50(3):606–9, 2008.
- [8] N. Guglielmi and E. Hairer. Classification of hidden dynamics in discontinuous dynamical systems. *SIADS*, 14(3):1454–1477, 2015.
- [9] O. Hájek. Discontinuous differential equations, I. *J. Differential Equations*, 32(2):149–170, 1979.
- [10] S. J. Hogan, M. E. Homer, M. R. Jeffrey, and R. Szalai. Piecewise smooth dynamical systems theory: the case of the missing boundary equilibrium bifurcations. *submitted*, 2015.
- [11] M. R. Jeffrey. Dynamics at a switching intersection: hierarchy, isonomy, and multiple-sliding. *SIADS*, 13(3):1082–1105, 2014.
- [12] M. R. Jeffrey. Hidden dynamics in models of discontinuity and switching. *Physica D*, 273-274:34–45, 2014.
- [13] M. R. Jeffrey. Hidden degeneracies in piecewise smooth dynamical systems. *submitted*, 2015.
- [14] M. R. Jeffrey and D. J. W. Simpson. Non-Filippov dynamics arising from the smoothing of nonsmooth systems, and its robustness to noise. *Nonlinear Dynamics*, 76(2):1395–1410, 2014.
- [15] M. A. Kiseleva and N. V. Kuznetsov. Coincidence of the gelig-leonov-yakubovich, filippov, and aizerman-pyatnitskiy definitions. *Vestnik St. Petersburg University: Mathematics*, 48(2):66–71, 2015.
- [16] P. Kowalczyk and P.T. Piiroinen. Two-parameter sliding bifurcations of periodic solutions in a dry-friction oscillator. *Physica D: Nonlinear Phenomena*, 237(8):1053 – 1073, 2008.
- [17] K. U. Kristiansen and S. J. Hogan. Regularizations of two-fold bifurcations in planar piecewise smooth systems using blow up. *submitted*, 2015.
- [18] Yu. A. Kuznetsov, S. Rinaldi, and A. Gragnani. One-parameter bifurcations in planar Filippov systems. *Int. J. Bif. Chaos*, 13:2157–2188, 2003.
- [19] G. A. Leonov and N. V. Kuznetsov. Hidden attractors in dynamical systems. from hidden oscillations in hilbert-kolmogorov, aizerman, and kalman problems to hidden chaotic attractor in chua circuits. *Int. J. Bif. Chaos*, 23(01):1330002, 2013.
- [20] J. Llibre, P. R. da Silva, and M. A. Teixeira. Study of singularities in nonsmooth dynamical systems via singular perturbation. *SIAM J. App. Dyn. Sys.*, 8(1):508–526, 2009.
- [21] A. Machina, R. Edwards, and P. van den Dreissche. Singular dynamics in gene network models. *SIADS*,

- 12(1):95–125, 2013.
- [22] D. N. Novaes and M. R. Jeffrey. Regularization of hidden dynamics in piecewise smooth flow. *J. Differ. Equ.*, 259:4615–4633, 2015.
- [23] S. H. Piltz, M. A. Porter, and P. K. Maini. Prey switching with a linear preference trade-off. *SIAM J. Appl. Math.*, 13(2):658–682, 2014.
- [24] E. Plahte and S. Kloglum. Analysis and generic properties of gene regulatory networks with graded response functions. *Physica D*, 201:150–176, 2005.
- [25] J. Sotomayor and M. A. Teixeira. Regularization of discontinuous vector fields. *Proceedings of the International Conference on Differential Equations, Lisboa*, pages 207–223, 1996.
- [26] M. A. Teixeira. Generic bifurcation of sliding vector fields. *J. Math. Anal. Appl.*, 176:436–457, 1993.
- [27] M. A. Teixeira and P. R. da Silva. Regularization and singular perturbation techniques for non-smooth systems. *Physica D*, 241(22):1948–55, 2012.
- [28] V. I. Utkin. Variable structure systems with sliding modes. *IEEE Trans. Automat. Contr.*, 22, 1977.
- [29] V. I. Utkin. *Sliding modes in control and optimization*. Springer-Verlag, 1992.
- [30] Various. Special issue on dynamics and bifurcations of nonsmooth systems. *Physica D*, 241(22):1825–2082, 2012.